The following publication M. Qu, T. Ding, Y. Sun, C. Mu, K. Pan and M. Shahidehpour, "Convex Hull Model for a Single-Unit Commitment Problem With Pumped Hydro Storage Unit," in IEEE Transactions on Power Systems, vol. 38, no. 5, pp. 4867-4880, Sept. 2023 is available at https://dx.doi.org/10.1109/TPWRS.2022.3215463.

Convex Hull Model for Single-Unit Commitment Problem with A Pump Storage Unit

Ming Qu, *Student Member, IEEE*, Tao Ding, *Senior Member, IEEE*, Chenggang Mu, *Student Member, IEEE*, Wenhao Jia, *Student Member, IEEE*, Kai Pan, *Member, IEEE*, Mohammad Shahidehpour, *Fellow, IEEE*

***Abstract*—The single-unit commitment (1UC) maximizes the revenue within a time series of given electricity prices while respecting generator-specific constraints, leading to a mixed-integer program (MIP). To reduce the computational complexity of the 1UC with a pump storage unit (PSU-1UC), we construct the convex hull of PSU-1UC in this paper. Focusing on the possible combination of alternating generation and pumping time intervals, we first establish a dynamic programming (DP) model that can be solved in polynomial time. Then, we reformulate the DP model into a linear programming (LP) model in a higher-dimensional space, which provides the convex hull of the PSU-1UC. It helps to speed up the large-scale unit commitment problems solved by decomposition algorithms from the perspective of formulation transformation. Numerical experiments demonstrate the effectiveness and efficiency of the proposed model.**

***Index Terms*—Single Unit Commitment, Convex Hull, Pump Storage Units, Lagrangian Relaxation**

I. Introduction

Unit commitment (UC) is a fundamental problem in power system operations [1-2]. The objective of UC is to minimize the total system operating cost on the premise of meeting both system-wide and generator-specific constraints [3]. It is a mixed-integer optimization model with a large number of binary decision variables, leading to an NP-hard problem. How to solve UC efficiently is still a hard nut to crack.

Mixed-integer programming (MIP) is the most widely used method to solve UC. The MIP-based security-constrained UC solution method was first described in [3]. Many advanced MIP algorithms have been gradually developed, such as branch-and-cut, which combines branch-and-bound and cutting plane methods in [4-6]. However, it is actually a systematic procedure based on “enumeration”.

As the number of units increases in power systems, the “curse of dimensionality” problem makes the UC harder to solve [7]. Thus, the decomposition algorithm has received much attention [8-13]. Lagrangian Relaxation (LR) is a traditional parallel method for large-scale instances when the computation time is prioritized. Ref. [8] decomposed a UC problem into several single-unit commitments (1UCs) by relaxing the coupling constraints (i.e., power balance constraints), and the solutions of all the 1UCs provided a lower bound of the optimal value. In [9], the UC problem was solved distributedly by the Surrogate Lagrangian relaxation (SLR) method [10], which overcame vibration as well as convergence difficulties. Ref. [11] provided an asynchronous decentralized solution framework for the unit commitment problem, which was solved by a two-phase algorithm according to the convex relaxation. By extending the ADMM method, [12] studied the method of solving large-scale distributed UC in a decentralized power network based on a multi-agent system. A fully parallel UC method was set up in [13] to obtain an efficient and fast solution for a large-scale power system, which decomposed the UC into multiple 1UC problems by the auxiliary problem principle.

According to the above decomposition methods, it can be found that the computational efficiency of 1UC is crucial since the 1UC serves as a subproblem of the original large-scale UC problems and is widely used for single-unit self-scheduling/ bidding problems [14].

The 1UC maximizes the revenue within a time series of given electricity prices while respecting generator-specific constraints. Ref. [15] established a two-stage algorithm for the 1UC with a thermal unit (TU-1UC) which can be solved in $O(T^3)$, where T is the number of dispatching periods. Its first stage was to find all the possible “on” periods with an optimal power output subsequence solved by dynamic programming. The second stage was to represent the TU-1UC as a graph whose nodes represent “on” periods weighted by corresponding optimal economic dispatching costs, and paths correspond to the binary decisions of the on/off state. Thus, TU-1UC was transformed into a shortest path problem. Refs. [16-17] further improved the method by reducing the computational time from $O(T^3)$ to $O(T^2)$, and derived extended tight formulations in the form of linear programming (LP) that can provide binary solutions. That means, the convex hull of the TU-1UC with binary variables was constructed, and the optimal solution can be obtained by using LP methods without combinatorial difficulties. Besides, Ref. [18] pointed out that the convex hull formulation could be used to improve and tighten the MIP formulation. Furthermore, the TU-1UC can be solved in polynomial time as a subproblem in the decomposition methods, and its convex hull formulation can be used to strengthen the MIP formulations, improving the computational performance.

In the field of hydraulic generation, the pump storage unit (PSU) is widely used in power systems as it improves the system flexibility by mitigating the active power fluctuations [19]. Thus, it is important to establish an appropriate hydrothermal UC model with PSUs [20,21] and solve it efficiently [22]. Ref. [20] proposed an MIP model for the hydrothermal UC, which showed that implementing PSUs can reduce operation costs. In [21], an interval hydrothermal UC model co-optimizing PSUs and the thermal units was proposed, which indicated that the PSU could significantly reduce renewable energy curtailment. To solve such a hydrothermal UC with PSUs efficiently, a decomposition algorithm was proposed in [22], combining the LR and Benders decomposition. The results showed that the reduced computational time becomes more evident as the number of PSUs or thermal units increases.

However, the acceleration algorithms in [14-17] are only designed for the TU-1UC, which cannot be applied to the 1UC with a PSU (PSU-1UC). Moreover, few studies focus on the acceleration algorithm for the PSU-1UC, which is important for solving the large-scale hydrothermal UC in the decomposition framework. To address the problem, this paper designs a dynamic programming model (DP) and reformulates it into an LP model, which provides the convex hull of the PSU-1UC. The contributions are summarized as follows

i) Focusing on the possible combinations of alternating generation and pumping time intervals, we establish a DP of the PSU-1UC with a general convex cost function. The proposed DP model can be solved in O(T^2L), where L is the time complexity of solving the convex economic dispatching (ED) problem of PSU with fixed binary variables.

ii) We further reformulate the DP model into an LP model in a higher-dimensional space, which can generate an optimal binary solution in polynomial time. Moreover, we have strictly proved that the optimal solution of the LP and the original MIP is equivalent, and the corresponding convex hull of such an NP-hard problem is constructed. Using the proposed convex hull model could lead to improvement in solving PSU-1UC.

The remainder of the paper is organized as follows: Section II presents an MIP model of PSU-1UC. In Section III, we design a DP model and construct the convex hull of the PSU-1UC. Section IV provides the analysis of case studies, and Section V concludes the paper.

II. MIP MODEL OF THE PSU-1UC MODEL

As shown in Fig.1, a PSU consists of an upstream reservoir, a downstream reservoir, a turbine, and a pump, which can either absorb or generate electricity. The PSU can undertake the tasks of peak load shifting in the power systems, releasing water from the upstream to downstream reservoirs to generate electricity by the turbine during peak load (the turbining state), and pumping water from the downstream to upstream reservoirs by the pump to consume electricity during the valley loads (the pumping state). The PSU can be operated in only one of the above two states at any time.

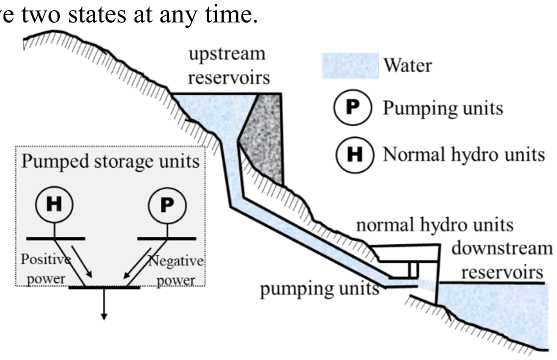

Fig.1 Schematic diagram of the pump storage station

For a PSU, both unit constraints and reservoir constraints should be considered. The PSU-1UC can be formed as follows

$$\min \sum_{t=1}^{T} (C^{up} u_t + C^{dn}(u_t + x_{t-1} - x_t) + f(P_t, Q_t, x_t)) \quad (1a)$$

The unit constraints include

$$x_t - x_{t-1} \le u_t, \ \ t \in [1,T]_{\mathbf{Z}} \quad (1b)$$

$$\sum_{i=t-T^p+1}^{t} u_i \le x_t, t \in [T^p, T]_{\mathbf{Z}} \quad (1c)$$

$$\sum_{i=t-T^q+1}^{t} u_i \le 1 - x_{t-T^q}, t \in [T^q, T]_{\mathbf{Z}} \quad (1d)$$

$$x_t P^{\min} \le P_t \le x_t P^{\max}, \ t \in [1,T]_{\mathbf{Z}} \quad (1e)$$

$$-(1-x_t) Q^{\max} \le Q_t \le 0, t \in [1,T]_{\mathbf{Z}} \quad (1f)$$

$$\left| P_t - P_{t-1} \right| \le V^p x_{t-1} + \overline{V^p}(1 - x_{t-1}), \ t \in [2,T]_{\mathbf{Z}} \quad (1g)$$

$$\left| Q_t - Q_{t-1} \right| \le V^q x_{t-1} + \overline{V^q}(1 - x_{t-1}), \ t \in [1,T]_{\mathbf{Z}} \quad (1h)$$

The reservoir constraints include

$$\underline{U^u} \le U_t^u \le \overline{U^u}, \forall t \quad (1i)$$

$$\underline{U^d} \le U_t^d \le \overline{U^d}, \forall t \quad (1j)$$

$$U_t^u - U_{t+1}^u = \eta^p P_t + \eta^q Q_t, t \in [1, T-1]_{\mathbf{Z}} \quad (1k)$$

$$U_{t+1}^d - U_t^d = \eta^p P_t + \eta^q Q_t, t \in [1, T-1]_{\mathbf{Z}} \quad (1l)$$

$$x_t, u_t \in \{0,1\}, P_t \ge 0, Q_t \le 0, U_t^u \ge 0, U_t^d \ge 0 \quad (1m)$$

where x_t is the binary variable indicating the turbining or pumping states at period t (if the PSU is turbining at time t, x_t=1; otherwise, x_t=0); u_t is the binary variable to indicate whether the turbine starts up at period t; P_t/Q_t represents the pumping/turbining power (P^{max}/P^{min} and Q^{max}/Q^{min} are upper/lower bounds of P_t and Q_t); T^p/T^q denotes the minimum-turbining/-pumping periods; V *and* $\overline{V}$ are the normal and startup ramp rate limits; U_t^u/U_t^d is the reservoir volume of upstream/ downstream reservoirs ($\underline{U^u}$ / $\overline{U^u}$ and $\underline{U^d}$ / $\overline{U^d}$ are upper/lower bounds of U_t^u and U_t^d); η^p/η^q denotes the conversion coefficient of water-to-electricity/electricity-to-water. Usually, the pump works in the interval of $Q_t \in [-Q^{\max}, 0]$ [23]. Thus, the shut-down state can be regarded as a special pumping state with $Q_t = 0$.

Constraint (1b) limits the operation status of the PSU. Constraints (1c)-(1d) restrict the minimum-puming/-turbining periods. Constraints (1e)-(1f) denote the limits on pumping/turbining powers. Constraints (1g)-(1h) specify the ramp-up/-down rate limits. Constraints (1i)-(1j) provide the upper and lower bounds of the reservoir volume. Constraints (1k)-(1l) represent the reservoir volume balance.

III. CONVEX HULL OF THE PSU-1UC MODEL

In this section, we first divide the whole dispatching interval [1,T] into all the possible combinations of several pumping and turbining time intervals. Each time interval is represented as a time-index pair (t,k). Then, taking all the possible pumping and turbining time intervals as the state space, a dynamic programming (DP) model is designed, which can be reformulated to an equivalent LP model whose feasible region is proved to be the convex hull of the PSU-1UC model.

A. Dynamic Programming of PSU-1UC Model

The PSU-1UC model aims to minimize operating costs. For each period t, we use a double-valued cost function ($\Omega^+(t)$ and $\Omega^-(t)$) to represent the operating costs from period t to the end. Specifically, as shown in Fig.2, $\Omega^+(t)$ represents the costs from period t to T when the PSU is pumping at period t-1 and is turbining in period t. $\Omega^{-}(t)$ represents the operating costs from period t to T when the PSU is turbining at period t-1 and is pumping at period t. Thus, the Bellman equation of the dynamic programming of the PSU-1UC model can be expressed as

$$\Omega^{+}(t)=\min_{k\in[\min\{t+T^{on}-1,T-1\},T-1]_{\mathbb{Z}}}\{C^{dn}+P(t,k)+\Omega^{-}(k),\ P(t,T)+\Omega^{-}(T)\},t\in[1,T]_{\mathbb{Z}} \tag{2a}$$

$$\Omega^{-}(t)=\min_{k\in[t+T^{q}+1,T]_{\mathbb{Z}}}\{C^{up}+Q(t+1,k-1)+\Omega^{+}(k),\ Q(t+1,T)\},t\in[T^{q},T-T^{q}-1]_{\mathbb{Z}} \tag{2b}$$

$$\Omega^{-}(t)=Q(t+1,T),t\in[T-T^{q},T]_{\mathbb{Z}} \tag{2c}$$

where $P(t,k)$/$Q(t,k)$ denotes the operating costs when the PSU is turbining/pumping during the time interval (t,k), which should meet the minimum-up constraints of both turbine and pump. $P(t,k)$ and $Q(t,k)$ are essentially the optimal values of the PSU-ED model if $x_t=\cdots=x_k=1$ and $x_t=\cdots=x_k=0$, respectively. For $P(t,k)$ and $Q(t,k)$, we define the set containing all the possible time pairs (t,k) as G and H, respectively, satisfying

$$\begin{aligned}&G=\{(t,k)\mid t\in[1,T]_{\mathbb{Z}},k\in[\min\{t+T^{p}-1,T\},T]_{\mathbb{Z}}\}\\&H=\{(t,k)\mid t=1,k\in[1,T]_{\mathbb{Z}}\}\\&\quad\bigcup\{(t,k)\mid t\in[T^{p}+1,T],k\in[\min\{t+T^{q}-1,T\},T]_{\mathbb{Z}}\}\end{aligned} \tag{3}$$

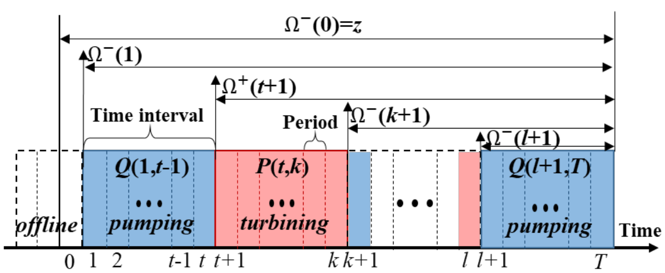

Fig.2 Optimal operation states of the PSU

Equation (2a) indicates that there are two operation modes after the PSU switches to the turbining state at time t: i) keeps the turbining state until period k, and then switches to the pumping state at period k+1; ii) keeps the turbining state to the end. Equation (2b) describes that, if $t\in[T^q, T-T^q-1]_z$, there are two operation modes after the PSU switches to the pumping state at period t+1: i) keeps the pumping state until period k-1, and then switches to the turbining state at period k; ii) keeps the pumping state to the end. Equation (2c) indicates that if PSU switches to the pumping state at period t+1($t\in[T-T^q, T]_z$), it can only keep pumping due to the limits of minimum-up periods.

Suppose that the PSU has been offline for s_0($s_0\geq T^q$) periods, the PSU-1UC model is equivalent to the following DP model

$$z=\Omega^{-}(0)=\min\{Q(1,t-1)+C^{up}+\Omega^{+}(t),Q(1,T)\} \tag{4}$$

Proposition 1: The proposed DP model (4) can be solved in O(T^2L), while the PSU-1UC model (1) can be solved in O($2^{2T}L$), where L is the time complexity of the PSU-ED model with fixed binary variables x_t and u_t.

Proof: We use the branch and bound (B&B) algorithm to solve the PSU-1UC model (1). The nodes of the complete binary tree grow exponentially, which means that we need to solve the PSU-ED for 2^{2T} times in the worst case. The time complexity of the B&B algorithm is O($2^{2T}L$).

In order to get the optimal value of the model (4), we should solve all the value functions $\Omega^{+}(t)$ and $\Omega^{-}(t)$, $t\in[1,T]$, which takes O(T). When we solve a certain value function at period t, we will calculate all the possible operating costs corresponding to different k for $k\leq T$. This means, at most T PSU-ED should be solved, which takes O(TL) at most. Therefore, The DP model (4) can be solved in O(T^2L).

(Q.E.D.)

The proposed DP for the PSU-1UC model significantly reduces the time complexity from $O(2^{2T}L)$ to $O(T^2L)$. More importantly, the DP model can be reformulated as an LP model whose feasible region is the convex hull of the PSU-1UC model. The details can be formulated as follows.

B. Convex Hull Model of the PSU-1UC

Taking the Bellman equations (2) and (4) as constraints, the model (4) can be reformulated as an LP model as

$$\max z \tag{5a}$$

s.t.

$$(\alpha_t)\ z\leq Q(1,t-1)+C^{up}+\Omega^{+}(t),\forall t\in[1,T]_{\mathbb{Z}} \tag{5b}$$

$$(\xi)\ z\leq Q(1,T) \tag{5c}$$

$$(\beta_{tk})\ \begin{aligned}&\Omega^{+}(t)\leq C^{dn}+P(t,k)+\Omega^{-}(k),\\&\forall k\in[\min\{t+T^{p}-1,T-1\},T-1]_{\mathbb{Z}},\forall t\in[1,T]_{\mathbb{Z}}\end{aligned} \tag{5d}$$

$$(\beta_{tk})\ \Omega^{+}(t)\leq P(t,T)+\Omega^{-}(T),t\in[1,T]_{\mathbb{Z}} \tag{5e}$$

$$(\gamma_{tk})\ \begin{aligned}&\Omega^{-}(t)\leq C^{up}+Q(t+1,k-1)+\Omega^{+}(k),\\&k\in[t+T^{q}+1,T]_{\mathbb{Z}},t\in[T^{q},T-T^{q}-1]_{\mathbb{Z}}\end{aligned} \tag{5f}$$

$$(\theta_t)\ \Omega^{-}(t)\leq Q(t+1,T),t\in[T-T^{q},T]_{\mathbb{Z}} \tag{5g}$$

where α_t, ξ, β_{tk}, γ_{tk}, θ_t are dual variables of corresponding constraints. Constraints (5a)-(5c) are equivalent to (4), constraints (5d)-(5e) correspond to (2a), and constraints (5f)-(5g) correspond to (2b)-(2c). Since $P(t,k)$ and $Q(t,k)$ are functions of state variables (P_s, Q_s, x_s), $s\in[t,k]$, the model (5) cannot be solved directly. If both $P(t,k)$ and $Q(t,k)$ are expressed as the corresponding ED models, and embedded into the model (5) as the supplementary constraints, then the LP model (5) can be solved.

The ED model corresponding to $P(t,k)$ is written as

$$P(t,k)=\min\sum\nolimits_{s=t}^{k}\phi_{tk,s}^{p} \tag{6a}$$

s.t.

$$(\lambda_{tk,s}^{p\mp})P^{\min}\leq y_{tk,s}^{p}\leq P^{\max},\forall s\in[t,k] \tag{6b}$$

$$(\mu_{tk,t}^{p})y_{tk,t}^{p}\leq\overline{V^{p}} \tag{6c}$$

$$(\mu_{tk,k}^{p})y_{tk,k}^{p}\leq\overline{V^{p}} \tag{6d}$$

$$(\sigma_{tk,s}^{p\mp})V^{p}\leq y_{tk,s-1}^{p}-y_{tk,s}^{p}\leq V^{p},\forall s\in[t+1,k] \tag{6e}$$

$$(\delta_{tk,s}^{p})\phi_{tk,s}^{p}-a_{s}^{p}y_{tk,s}\geq b^{p},\forall s\in[t,k] \tag{6f}$$

$$(\omega_{tk,s}^{pu})U_{tk,s-1}^{pu}-U_{tk,s}^{pu}=\eta^{p}y_{tk,s-1}^{p},\forall s\in[t+1,k] \tag{6g}$$

$$(\varepsilon_{tk,s}^{pu\mp})\underline{U^{pu}}\leq U_{tk,s}^{pu}\leq\overline{U^{pu}},\forall s\in[t,k] \tag{6h}$$

$$(\omega_{tk,s}^{pd})U_{tk,s}^{pd}-U_{tk,s-1}^{pd}=\eta x_{tk,s-1}^{p},\forall s\in[t+1,k] \tag{6i}$$

$$(\varepsilon_{tk,s}^{pd\mp})\underline{U^{pd}}\leq U_{tk,s}^{pd}\leq\overline{U^{pd}},\forall s\in[t,k] \tag{6j}$$

The ED model corresponding to $Q(t,k)$ is written as

$$Q(t,k)=\min\sum_{s=t}^{k}\phi^{q}_{tk,s} \tag{7a}$$

s.t.

$$(\lambda^{q\mp}_{tk,s})Q^{\min}\le y^{q}_{tk,s}\le Q^{\max},\forall s\in[t,k] \tag{7b}$$

$$(\mu^{q}_{tk,t})y^{q}_{tk,t}\le\overline{V^{q}} \tag{7c}$$

$$(\mu^{q}_{tk,k})y^{q}_{tk,k}\le\overline{V^{q}} \tag{7d}$$

$$(\sigma^{q\mp}_{tk,s})-V^{q}\le y^{q}_{tk,s}-y^{q}_{tk,s-1}\le V^{q},\forall s\in[t+1,k] \tag{7e}$$

$$(\delta^{q}_{tk,s})\phi^{q}_{tk,s}\ge\pi_{s}y^{q}_{tk,s},\forall s\in[t,k] \tag{7f}$$

$$(\omega^{qu}_{tk,s})U^{qu}_{tk,s-1}-U^{qu}_{tk,s}=\eta^{q}y^{q}_{tk,s\text{-}1},\forall s\in[t+1,k] \tag{7g}$$

$$(\varepsilon^{qu\mp}_{tk,s})\underline{U^{qu}}\le U^{qu}_{tk,s}\le\overline{U^{qu}},\forall s\in[t,k] \tag{7h}$$

$$(\omega^{qd}_{tk,s})U^{qd}_{tk,s}-U^{qd}_{tk,s-1}=\eta^{q}y^{q}_{tk,s\text{-}1},\forall s\in[t+1,k] \tag{7i}$$

$$(\varepsilon^{qd\mp}_{tk,s})\underline{U^{qd}}\le U^{qd}_{tk,s}\le\overline{U^{qd}},\forall s\in[t,k] \tag{7j}$$

where on the left side of each constraint is the dual variable, y denotes the pumping/turbining powers, and U represents the reservoir volume. For all the variables, the superscripts "u" and "d" denote upstream and downstream reservoirs, respectively; superscripts "p" and "q" indicate the turbining and pumping, respectively; subscript "tk,s" indicates the s-th ($t\le s\le k$) period during the time interval (t,k). Constraints (6b) and (7b) limit the outputs. Constraints (6c)-(6e) and (7c)-(7e) specify the ramp-up/-down rate limits. Constraints (6g),(6i),(7g), and (7i) represent the reservoir volume balance. Constraints (6h), (6j), (7h), and (7j) provide the upper/lower bounds of the reservoir volume. The models (6) and (7) obviously meet the minimum-up constraints with the given (t,k). When k=T, (6d) and (7d) can be omitted because the state at the T+1 period is not considered.

Note that the model (5) is a maximization problem, while $P(t,k)$ and $Q(t,k)$ are minimization problems. To embed the models (6) and (7) into the model (5), we leverage the dual formulation of the models (6) and (7), which gives maximization problems as follows

$$\begin{aligned}P(t,k)=\max&\sum_{s=t}^{k}(\lambda^{p+}_{tk,s}P^{\max}-\lambda^{p-}_{tk,s}P^{\min})+\sum_{s=t}^{k}b^{p}\delta^{p}_{tk,s}\\&+\overline{V^{p}}(\mu^{p}_{tk,t}+\mu^{p}_{tk,k})+\sum_{s=t+1}^{k}V^{p}(\sigma^{p+}_{tk,s}+\sigma^{p-}_{tk,s})\\&+\sum_{s=t}^{k}\Big[(\varepsilon^{\text{pu}+}_{tk,s}+\varepsilon^{\text{pd}+}_{tk,s})\overline{U^{u}}-(\varepsilon^{\text{pu-}}_{tk,s}+\varepsilon^{\text{pd-}}_{tk,s})\underline{U^{d}}\Big]\end{aligned} \tag{8a}$$

s.t.

$$(p_{tk,t})\begin{array}{l}\lambda^{p+}_{tk,t}-\lambda^{p-}_{tk,t}+\mu^{p}_{tk,t}-\sigma^{p+}_{tk,t+1}+\sigma^{p-}_{tk,t+1}\\\quad-a^{p}\delta^{p}_{tk,t}+\eta^{p}(\omega^{pu}_{tk,t+1}+\omega^{pd}_{tk,t+1})=0\end{array} \tag{8b}$$

$$(p_{tk,s})\begin{array}{l}\lambda^{p+}_{tk,s}-\lambda^{p-}_{tk,s}+\sigma^{p+}_{tk,s}-\sigma^{p+}_{tk,s+1}-\sigma^{p-}_{tk,s}+\sigma^{p-}_{tk,s+1}-a^{p}\delta^{p}_{tk,s}\\+\eta^{p}(\omega^{pu}_{tk,s+1}+\omega^{pd}_{tk,s+1})=0,\forall s\in[t+1,k-1]\end{array} \tag{8c}$$

$$(p_{tk,k})\ \lambda^{p+}_{tk,k}-\lambda^{p-}_{tk,k}+\mu^{p}_{tk,k}-\sigma^{p+}_{tk,k}+\sigma^{p-}_{tk,k}-a^{p}\delta^{p}_{tk,k}=0 \tag{8d}$$

$$(\kappa^{p}_{tk,s})\delta^{p}_{tk,s}=1,\forall s\in[t,k] \tag{8e}$$

$$(\vartheta^{u}_{tk,t})\varepsilon^{pu+}_{tk,t}-\varepsilon^{pu\text{-}}_{tk,t}+\omega^{pu}_{tk,t+1}=0 \tag{8f}$$

$$(\vartheta^{u}_{tk,s})\varepsilon^{pu+}_{tk,s}-\varepsilon^{pu\text{-}}_{tk,s}-\omega^{pu}_{tk,s}+\omega^{pu}_{tk,s+1}=0,\forall s\in[t+1,k-1] \tag{8g}$$

$$(\vartheta^{u}_{tk,k})\varepsilon^{pu+}_{tk,k}-\varepsilon^{pu\text{-}}_{tk,k}-\omega^{pu}_{tk,k}=0 \tag{8h}$$

$$(\vartheta^{d}_{tk,t})\varepsilon^{pd+}_{tk,t}-\varepsilon^{pd\text{-}}_{tk,t}-\omega^{pd}_{tk,t+1}=0 \tag{8i}$$

$$(\vartheta^{d}_{tk,s})\varepsilon^{pu+}_{tk,s}-\varepsilon^{pu\text{-}}_{tk,s}+\omega^{pu}_{tk,s}-\omega^{pu}_{tk,s+1}=0,\forall s\in[t+1,k-1] \tag{8j}$$

$$(\vartheta^{d}_{tk,k})\varepsilon^{pd+}_{tk,k}-\varepsilon^{pd\text{-}}_{tk,k}+\omega^{pd}_{tk,k+1}=0 \tag{8k}$$

$$\lambda^{p\pm}_{tk,s},\mu^{p}_{tk,s},\sigma^{p\pm}_{tk,s},\varepsilon^{pu\pm}_{tk,s},\varepsilon^{pd\pm}_{tk,s}\le 0,\forall s \tag{8l}$$

$$\begin{aligned}Q(t,k)=\max&\sum_{s=t}^{k}(\lambda^{q+}_{tk,s}Q^{\max}-\lambda^{q-}_{tk,s}Q^{\min})\\&+\overline{V^{q}}(\mu^{q}_{tk,t}+\mu^{q}_{tk,k})+\sum_{s=t+1}^{k}V^{q}(\sigma^{q+}_{tk,s}+\sigma^{q-}_{tk,s})\\&+\sum_{s=t}^{k}\Big[(\varepsilon^{qu+}_{tk,s}+\varepsilon^{qu+}_{tk,s})\overline{U^{u}}-(\varepsilon^{qu\text{-}}_{tk,s}+\varepsilon^{qd\text{-}}_{tk,s})\underline{U^{d}}\Big]\end{aligned} \tag{9a}$$

s.t.

$$(q_{tk,t})\begin{array}{l}\lambda^{q+}_{tk,t}-\lambda^{q-}_{tk,t}+\mu^{q}_{tk,t}-\sigma^{q+}_{tk,t+1}+\sigma^{q-}_{tk,t+1}\\\quad-\pi_{t}\delta^{q}_{tk,t}+\eta^{q}(\omega^{qu}_{tk,t+1}+\omega^{qd}_{tk,t+1})=0\end{array} \tag{9b}$$

$$(p_{tk,s})\begin{array}{l}\lambda^{q+}_{tk,s}-\lambda^{q-}_{tk,s}+\sigma^{q+}_{tk,s}-\sigma^{q+}_{tk,s+1}-\sigma^{q-}_{tk,s}+\sigma^{q-}_{tk,s+1}-\pi_{s}\delta^{q}_{tk,s}\\+\eta^{q}(\omega^{qu}_{tk,s+1}+\omega^{qd}_{tk,s+1})=0,\forall s\in[t+1,k-1]\end{array} \tag{9c}$$

$$(q_{tk,k})\ \lambda^{q+}_{tk,k}-\lambda^{q-}_{tk,k}+\mu^{q}_{tk,k}-\sigma^{q+}_{tk,k}+\sigma^{q-}_{tk,k}-\pi_{k}\delta^{q}_{tk,k}=0 \tag{9d}$$

$$(\kappa^{q}_{tk,s})\delta^{q}_{tk,s}=1,\forall s\in[t,k] \tag{9e}$$

$$(o^{u}_{tk,t})\varepsilon^{qu+}_{tk,t}-\varepsilon^{qu\text{-}}_{tk,t}+\omega^{qu}_{tk,t+1}=0 \tag{9f}$$

$$(o^{u}_{tk,s})\varepsilon^{qu+}_{tk,s}-\varepsilon^{qu\text{-}}_{tk,s}-\omega^{qu}_{tk,s}+\omega^{qu}_{tk,s+1}=0,\forall s\in[t+1,k-1] \tag{9g}$$

$$(o^{u}_{tk,k})\varepsilon^{qu+}_{tk,k}-\varepsilon^{qu\text{-}}_{tk,k}-\omega^{qu}_{tk,k}=0 \tag{9h}$$

$$(o^{d}_{tk,t})\varepsilon^{qd+}_{tk,t}-\varepsilon^{qd\text{-}}_{tk,t}-\omega^{qd}_{tk,t+1}=0 \tag{9i}$$

$$(o^{d}_{tk,s})\varepsilon^{qd+}_{tk,s}-\varepsilon^{qd\text{-}}_{tk,s}+\omega^{qd}_{tk,s}-\omega^{qd}_{tk,s+1}=0,\forall s\in[t+1,k-1] \tag{9j}$$

$$(o^{d}_{tk,s})\varepsilon^{qd+}_{tk,k}-\varepsilon^{qd\text{-}}_{tk,k}+\omega^{qd}_{tk,k+1}=0 \tag{9k}$$

$$\lambda^{q\pm}_{tk,s},\mu^{q}_{tk,s},\sigma^{q\pm}_{tk,s},\varepsilon^{qu\pm}_{tk,s},\varepsilon^{qd\pm}_{tk,s}\le 0,\forall s \tag{9l}$$

For PSU-1UC with energy coupling constraints (i.e., the reservoir volume balance constraints (1i)-(1k)), the operation state (P_t, Q_t, x_t, u_t) in any time interval (t,k) must be coupled with the operation state in the previous possible time interval (*, t-1) and the latter possible time interval (k+1, *). The symbol "*" represents all the possible periods that satisfy the minimum-up constraints. Taking $P(t,k)$ as an example, in the model (8), $P(t,k)$ is independent and not affected by other $P(t',k')$ or $Q(t',k')$. This is because that constraints (6g) and (6j) cannot describe the coupling relationship between $U^{pu}_{tk,k}$ and $U^{qu}_{(k+1)*,k+1}$, which belong to different time intervals. This leads to the lack of coupling relationship between the last period k and the subsequent period k+1 in (8d), (8h), and (8k).

To describe the coupling relationship between different consecutive time intervals, we define a set of public variables Λ^{pu}_{k}, Λ^{pd}_{k}, Π^{pu}_{k}, and Π^{pd}_{k}, which should be embedded into (8d), (8f), (8h), (8i), and (8k) of all the $P(*,k)$ as follows

$$(p_{tk,k})\ \lambda^{p+}_{tk,k}-\lambda^{p-}_{tk,k}+\mu^{p}_{tk,k}-\sigma^{p+}_{tk,k}+\sigma^{p-}_{tk,k}-a^{p}\delta^{p}_{tk,k}+\eta^{p}(\Lambda^{pu}_{k}+\Lambda^{pd}_{k})=0 \tag{10a}$$

$$(\vartheta^{u}_{tk,t})\varepsilon^{pu+}_{tk,t}-\varepsilon^{pu\text{-}}_{tk,t}-\Pi^{pu}_{t}+\omega^{pu}_{tk,t+1}=0 \tag{10b}$$

$$(\vartheta^{u}_{tk,k})\varepsilon^{pu+}_{tk,k}-\varepsilon^{pu\text{-}}_{tk,k}-\omega^{pu}_{tk,k}+\Pi^{pu}_{k}=0 \tag{10c}$$

$$(\vartheta^{d}_{tk,k})\varepsilon^{pd+}_{tk,t}-\varepsilon^{pd-}_{tk,t}-\omega^{pd}_{tk,t+1}+\Pi^{pd}_{t}=0 \tag{10d}$$

$$(\vartheta^{d}_{tk,k})\varepsilon^{pd+}_{tk,k}-\varepsilon^{pd-}_{tk,k}-\Pi^{pd}_{k}+\omega^{pd}_{tk,k+1}=0 \tag{10e}$$

Similarly, we define a set of public variables $\Lambda^{qu}_k, \Lambda^{qd}_k$, Π^{qu}_k, and Π^{qd}_k for all the $Q(*, k)$, and (9d), (9f), (9h), (9i), and (9k) can be reformulated as

$$(q_{tk,k})\ \lambda^{q+}_{tk,k}-\lambda^{q-}_{tk,k}+\mu^{q}_{tk,k}-\sigma^{q+}_{tk,k}+\sigma^{q-}_{tk,k}-\pi_k\delta^{q}_{tk,k}-\eta^{q}(\Lambda^{qu}_k-\Lambda^{qd}_k)=0 \tag{11a}$$

$$(o^{u}_{tk,t})\varepsilon^{qu+}_{tk,t}-\varepsilon^{qu-}_{tk,t}+\omega^{qu}_{tk,t+1}+\Pi^{qu}_{t}=0 \tag{11b}$$

$$(o^{u}_{tk,k})\varepsilon^{qu+}_{tk,k}-\varepsilon^{qu-}_{tk,k}-\omega^{qu}_{tk,k}-\Pi^{qu}_{k}=0 \tag{11c}$$

$$(o^{d}_{tk,t})\varepsilon^{qd+}_{tk,t}-\varepsilon^{qd-}_{tk,t}-\omega^{qd}_{tk,t+1}-\Pi^{qd}_{t}=0 \tag{11d}$$

$$(o^{d}_{tk,s})\varepsilon^{qd+}_{tk,k}-\varepsilon^{qd-}_{tk,k}+\omega^{qd}_{tk,k+1}+\Pi^{qd}_{k}=0 \tag{11e}$$

It can be concluded that considering the energy coupling relationship for all the possible turbining intervals and the pumping intervals, (8) and (10) are the dual formulation of the ED model (6) corresponding to $P(t,k)$; (9) and (11) are the dual formulation of the ED model (7) corresponding to $Q(t,k)$. Embedding $P(t,k)$ and $Q(t,k)$, i.e., (8)-(11), into (5), the PSU-1UC is formulated as an LP, yielding

$$\max z \tag{12a}$$

s.t.

(5b)-(5g) (12b)

$$(\zeta_{tk})\quad \begin{aligned} P(t,k) \le {} & \sum_{s=t}^{k}(\lambda^{p+}_{tk,s}\overline{C^{p}}-\lambda^{p-}_{tk,s}\underline{C^{p}})+\sum_{s=t}^{k}b^{p}\delta^{p}_{tk,s} \\ & +\overline{V^{p}}(\mu^{p}_{tk,t}+\mu^{p}_{tk,k})+\sum_{s=t+1}^{k}V^{p}(\sigma^{p+}_{tk,s}+\sigma^{p-}_{tk,s}) \\ & +\sum_{s=t}^{k}\Big[(\varepsilon^{\text{pu+}}_{tk,s}+\varepsilon^{\text{pd+}}_{tk,s})\overline{U^{u}}-(\varepsilon^{\text{pu-}}_{tk,s}+\varepsilon^{\text{pd-}}_{tk,s})\underline{U^{d}}\Big] \\ & \forall k\in[\min\{t+T^{p}-1,T-1\},T-1],\ \forall t\in[1,T] \end{aligned} \tag{12c}$$

$$(\zeta_{tT})\quad \begin{aligned} P(t,T) \le {} & \sum_{s=t}^{T}(\lambda^{p+}_{tk,s}\overline{C^{p}}-\lambda^{p-}_{tk,s}\underline{C^{p}})+\sum_{s=t}^{T}b^{p}\delta^{p}_{tk,s} \\ & +\overline{V^{p}}\mu^{p}_{tk,t}+\sum_{s=t+1}^{k}V^{p}(\sigma^{p+}_{tk,s}+\sigma^{p-}_{tk,s}) \\ & +\sum_{s=t}^{k}\Big[(\varepsilon^{\text{pu+}}_{tk,s}+\varepsilon^{\text{pd+}}_{tk,s})\overline{U^{u}}-(\varepsilon^{\text{pu-}}_{tk,s}+\varepsilon^{\text{pd-}}_{tk,s})\underline{U^{d}}\Big] \\ & \forall k\in[\min\{t+T^{p}-1,T-1\},T-1],\ \forall t\in[1,T] \end{aligned} \tag{12d}$$

(8a)-(8c),(8e),(8g),(8j),(8l),(10a)-(10e) (12e)

$$(\psi_{1k})\quad \begin{aligned} Q(1,k) \le {} & \sum_{s=1}^{t}(\lambda^{q+}_{s}\overline{C^{q}}-\lambda^{q-}_{s}\underline{C^{q}})+\overline{V^{q}}(\mu^{q}_{t}+\mu^{q}_{k}) \\ & +\sum_{s=t}^{k}\Big[(\varepsilon^{qu+}_{s}+\varepsilon^{qu+}_{s})\overline{U^{u}}-(\varepsilon^{qu-}_{s}+\varepsilon^{qd-}_{s})\underline{U^{d}}\Big] \\ & +\sum_{s=t+1}^{k}V^{q}(\sigma^{q+}_{s}+\sigma^{q-}_{s}),k\in[1,T] \end{aligned} \tag{12f}$$

$$(\psi_{tk})\quad \begin{aligned} Q(t,k) \le {} & \sum_{s=t}^{k}(\lambda^{q+}_{s}\overline{C^{q}}-\lambda^{q-}_{s}\underline{C^{q}}) \\ & +\overline{V^{q}}(\mu^{q}_{t}+\mu^{q}_{k})+\sum_{s=t+1}^{k}V^{q}(\sigma^{q+}_{s}+\sigma^{q-}_{s}) \\ & +\sum_{s=t}^{k}\Big[(\varepsilon^{qu+}_{s}+\varepsilon^{qu+}_{s})\overline{U^{u}}-(\varepsilon^{qu-}_{s}+\varepsilon^{qd-}_{s})\underline{U^{d}}\Big], \\ & k\in[t+T^{q},T-1],\ t\in[T^{q}+1,T-T^{q}] \end{aligned} \tag{12g}$$

$$(\psi_{tk})\quad \begin{aligned} Q(t,T) \le {} & \sum_{s=t}^{T}(\lambda^{q+}_{s}\overline{C^{q}}-\lambda^{q-}_{s}\underline{C^{q}})+\overline{V^{q}}(\mu^{q}_{t}) \\ & +\sum_{s=t}^{k}\Big[(\varepsilon^{qu+}_{s}+\varepsilon^{qu+}_{s})\overline{U^{u}}-(\varepsilon^{qu-}_{s}+\varepsilon^{qd-}_{s})\underline{U^{d}}\Big] \\ & +\sum_{s=t+1}^{k}V^{q}(\sigma^{q+}_{s}+\sigma^{q-}_{s}),t\in[T-T^{q}+1,T] \end{aligned} \tag{12h}$$

(9a)-(9c),(9e),(9g),(9j),(9l),(11a)-(11e) (12i)

The model (12) is the dual formulation of the model (1). Although the optimal values of the two models are the same, their optimal solutions are different because the decision variables of the two models are different. We are concerned about the solutions to decision variables (P_t, Q_t, x_t, u_t, U^u_t, U^d_t) in the original optimization model (5). However, the model (12) does not directly reflect the information of (P_t, Q_t, x_t, u_t, U^u_t, U^d_t), while only giving the information of dual variables. To find the optimal solution of the original optimization model (5), we have to take the dual formulation of (12) as

$$\min\sum_{t=1}^{T}C^{up}\alpha_t+\sum_{t=1}^{T}\sum_{k=t+T^{p}-1}^{T-1}C^{dn}\beta_{tk}+\sum_{t=T^{p}}^{t-T^{q}-1}\sum_{k=t+T^{q}+1}^{T}C^{up}\gamma_{tk}+\sum_{tk\in G}\sum_{s=t}^{k}\kappa^{p}_{tk,s}+\sum_{tk\in H}\sum_{s=t}^{k}\kappa^{q}_{tk,s} \tag{13a}$$

s.t.

$$\xi+\sum_{t=1}^{T}\alpha_t=1 \tag{13b}$$

$$\alpha_t-\sum_{k=\min\{t+T^{p}-1,T\}}^{T}\beta_{tk}+\sum_{k=T^{p}}^{T-T^{q}-1}\gamma_{kt}=0,\forall t\in[1,T] \tag{13c}$$

$$\theta_t-\sum_{k=1}^{t-T^{q}+1}\beta_{kt}+\sum_{k=t+T^{q}+1}^{T}\gamma_{tk}=0,\forall t\in[T^{on},T-T^{q}-1] \tag{13d}$$

$$\theta_t-\sum_{k=1}^{t-T^{q}+1}\beta_{kt}=0,\forall t\in[T-T^{q},T] \tag{13e}$$

$$\beta_{tk}=\zeta_{tk},\forall tk\in G \tag{13f}$$

$$\alpha_{t+1}=\psi_{1t},\xi=\psi_{1T},\forall t\in[2,T-1] \tag{13g}$$

$$\psi_{t+1,k-1}=\gamma_{tk},k\in[t+T^{q}+1,T],t\in[T^{on},T-T^{q}-1] \tag{13h}$$

$$\psi_{t+1,T}=\theta_t,t\in[T^{q},T] \tag{13i}$$

$$\zeta_{tk}P^{\min}\le p_{tk,s}\le\zeta_{tk}P^{\max},\forall s\in[t,k],\forall tk\in G \tag{13j}$$

$$p_{tk,t}\le\zeta_{tk}\overline{V^{p}},p_{tk,k}\le\zeta_{tk}\overline{V^{p}},\forall tk\in G \tag{13k}$$

$$-\zeta_{tk}V^{p}\le p_{tk,s-1}-p_{tk,s}\le\zeta_{tk}V^{p},\forall s\in[t{+}1,k],\forall tk\in G \tag{13l}$$

$$\kappa^{p}_{tk,s}\ge a^{p}p_{tk,s}+b^{p}\zeta_{tk},\forall s\in[t{+}1,k],\forall tk\in G \tag{13m}$$

$$\begin{aligned} &\zeta_{tk}\underline{U^{u}}\le\vartheta^{u}_{tk,s}\le\zeta_{tk}\overline{U^{u}},\forall tk\in G \\ &\zeta_{tk}\underline{U^{d}}\le\vartheta^{d}_{tk,s}\le\zeta_{tk}\overline{U^{d}},\forall tk\in G \end{aligned} \tag{13n}$$

$$\begin{aligned} &\vartheta^{u}_{tk,s-1}-\vartheta^{u}_{tk,s}=\eta^{p}p_{tk,s-1},\forall s\in[t{+}1,k],\forall tk\in G \\ &\vartheta^{d}_{tk,s-1}-\vartheta^{d}_{tk,s}=\eta^{p}p_{tk,s-1},\forall s\in[t{+}1,k],\forall tk\in G \end{aligned} \tag{13o}$$

$$\psi_{tk}Q^{\min}\le q_{tk,s}\le\psi_{tk}Q^{\max},\forall s\in[t,k],\forall tk\in H \tag{13p}$$

$$q_{tk,t}\le\psi_{tk}\overline{V^{q}},q_{tk,k}\le\psi_{tk}\overline{V^{q}},\forall tk\in H \tag{13q}$$

$$-\psi_{tk}V^{p}\le q_{tk,s-1}-q_{tk,s-1}\le\psi_{tk}V^{p},\forall s\in[t{+}1,k],\forall tk\in H \tag{13r}$$

$$\kappa^{q}_{tk,s}\ge\pi q_{tk,s},\forall s\in[t{+}1,k],\forall tk\in H \tag{13s}$$

$$\psi_{tk}\underline{U^u} \le o^u_{tk,s} \le \psi_{tk}\overline{U^u}, \forall tk \in H$$
$$\psi_{tk}\underline{U^d} \le o^d_{tk,s} \le \psi_{tk}\overline{U^d}, \forall tk \in H \tag{13t}$$

$$o^u_{tk,s-1} - o^u_{tk,s} = \eta^q q_{tk,s-1}, \forall s \in [t+1,k], \forall tk \in H$$
$$o^d_{tk,s-1} - o^d_{tk,s} = \eta^q q_{tk,s-1}, \forall s \in [t+1,k], \forall tk \in H \tag{13u}$$

$$\sum_{k=1}^{t-T^{off}+1}\left(o^u_{kt,t} - \eta^q q_{kt,t}\right) = \sum_{k=\min\{t+T^{on},T\}}^{T} \vartheta^u_{t+1,k,t+1}, \forall t \in [1,T-1] \tag{13v}$$

$$\sum_{k=1}^{t-T^{on}+1}\left(\vartheta^u_{kt,t} - \eta^p p_{kt,t}\right) = \sum_{k=\min\{t+T^{off},T\}}^{T} o^u_{t+1,k,t+1}, \forall t \in [1,T-1] \tag{13w}$$

$$\sum_{k=1}^{t-T^{off}+1}\left(o^d_{kt,t} + \eta^q q_{kt,t}\right) = \sum_{k=\min\{t+T^{on},T\}}^{T} \vartheta^d_{t+1,k,t+1}, \forall t \in [1,T-1] \tag{13x}$$

$$\sum_{k=1}^{t-T^{off}+1}\left(\vartheta^d_{kt,t} + \eta^p p_{kt,t}\right) = \sum_{k=\min\{t+T^{off},T\}}^{T} o^d_{t+1,k,t+1}, \forall t \in [1,T-1] \tag{13y}$$

$$\alpha_t,\ \xi,\ \beta_{tk},\ \gamma_{tk},\ \theta_t,\ \zeta_{tk},\ \psi_{tk} \ge 0 \tag{13z}$$

where constraints (13b)-(13i) describe the logical relationship among the binary variables α_t, ξ, β_{tk}, γ_{tk}, θ_t, ζ_{tk}, and ψ_{tk}; constraints (13j)-(13o) represent the physical constraints when the PSU is turbining, while (13p)-(13u) describe the physical constraints when the PSU is pumping; constraints (13v)-(13y) indicate the reservoir volume balance between consecutive time intervals, whose dual variables are the proposed public variables corresponding to the reservoir volume balance constraints between consecutive time intervals ($\Lambda^{pu}_k, \Lambda^{pd}_k$, Π^{pu}_k, Π^{pd}_k, $\Lambda^{qu}_k, \Lambda^{qd}_k$, Π^{qu}_k, and Π^{qd}_k).

Therefore, we obtain a polyhedron restricted by linear constraints. The extreme points of the polyhedron are binary for the decision variables α_t, ξ, β_{tk}, γ_{tk}, θ_t, ζ_{tk}, and ψ_{tk}. That is, for any linear or piecewise-linear convex objective function, the feasible region of the model (13) constructs the convex hull of the model (1), which will be proved in the following.

Proposition 2: For any linear or piecewise-linear objective function, the optimal solutions are binaries with respect to α_t, ξ, β_{tk}, γ_{tk}, θ_t, ζ_{tk}, and ψ_{tk}. The polyhedron provided by the model (13) is the convex hull of the model (1).

Proof: We prove Proposition 2 from the two aspects: **feasibility** and **optimality**. Specifically, with any linear or piecewise-linear objective function, the optimal solution of the model (1) is both the feasible and optimal solution of the model (13).

Suppose that the optimal solution of the model (1) is (P^*_t, Q^*_t, x^*_t, u^*_t, U^{u*}_t, U^{d*}_t), which determines a specific turbining/ pumping power, turbining/pumping state, and reservoir volume of the PSU at each period. Based on this optimal solution, we construct an optimal solution (α^*_t, ξ^*, β^*_{tk}, γ^*_{tk}, θ^*_t, $p^*_{tk,s}$, $q^*_{tk,s}$, $\vartheta^d_{tk,s}$, $\vartheta^u_{tk,s}$, $o^d_{tk,s}$, $o^u_{tk,s}$) by the following rules in Table I.

TABLE I. Construction rules of the variables in the model (13)

Var	Constructing rules
α^*_t	α^*_t=1 if the PSU keeps pumping from period 1 to the period t-1, and switches to the turbining state in period t; α^*_t =0 otherwise
ξ^*	ξ^* =1 if the PSU keeps pumping from period 1 to the end; ξ^* =0 otherwise
β^*_{tk} ζ^*_{tk}	$\beta^*_{tk}(\zeta^*_{tk})$=1 if the PSU keeps turbining during the time interval (t,k), and is pumping in period t-1 and period k+1; $\beta^*_{tk}(\zeta^*_{tk})$=0 otherwise
γ^*_{tk} $\psi^*_{t+1,k-1}$	$\gamma^*_{tk}(\psi^*_{t+1,k-1})$=1 if the PSU keeps pumping during time interval (t+1,k-1), and is in the turbining state in period t and period k; $\gamma^*_{tk}(\psi^*_{t+1,k-1})$=0 otherwise
θ^*_t	θ^*_t=1 if the PSU switches to the pumping state and keeps pumping during time interval (t+1,T), θ^*_t=0 otherwise
$p^*_{tk,s}$	$p^*_{tk,s}(p^*_{tk,s}\ge 0)$ takes the value of optimal generation amount for each s($t\le s\le k$) when the PSU keeps turbining during the time interval (t,k); $p^*_{tk,s}$=0 otherwise
$q^*_{tk,s}$	$q^*_{tk,s}(p^*_{tk,s} \le 0)$ takes the value of optimal power consumption for each s($t\le s\le k$) when the PSU keeps pumping during the time interval (t,k); $q^*_{tk,s}$=0 otherwise
$\vartheta^d_{tk,s}$/ $\vartheta^u_{tk,s}$	$\vartheta^d_{tk,s}/\vartheta^u_{tk,s}$ takes the value of down-/up-stream reservoir volume for each s($t\le s\le k$) when the PSU keeps turbining during the time interval (t,k); $\vartheta^d_{tk,s}/\vartheta^u_{tk,s}$ =0 otherwise
$o^d_{tk,s}/o^u_{tk,s}$	$o^d_{tk,s}/o^u_{tk,s}$ takes the value of down-/up-stream reservoir volume for each s($t\le s\le k$) when the PSU keeps pumping during the time interval (t,k); $o^d_{tk,s}/o^u_{tk,s}$ =0 otherwise

There are three operation modes of the PSU: i) only containing pumping state (i.e., PSU is pumping for all the periods); ii) only containing turbining state (i.e., PSU is turbining for all the periods); iii) containing both pumping and turbining states (i.e., PSU pumps at some periods while turbining at the other periods, but pumping and turbining shouldn't work simultaneously).

***Feasibility*:** A solution (α^*_t, ξ^*, β^*_{tk}, γ^*_{tk}, θ^*_t, $p^*_{tk,s}$, $q^*_{tk,s}$, $\vartheta^d_{tk,s}$, $\vartheta^u_{tk,s}$, $o^d_{tk,s}$, $o^u_{tk,s}$) can always be constructed, which characterizes the same dispatching scheme as (P^*_t, Q^*_t, x^*_t, u^*_t, U^{u*}_t, U^{d*}_t) and meets (13b)-(13z).

1) The first mode:

For this mode, $\forall \alpha^*_t$, β^*_{tk}, γ^*_{tk}, θ^*_t =0 except for ξ^*=1. Thus, constraints (13b)-(13e) are satisfied.

2) The second mode

For this mode, $\forall \xi^*$, γ^*_{tk}, θ^*_t =0 except for α^*_1, $\beta^*_{1,T}$=1. Thus, constraints (13b)-(13e) are satisfied.

3) The third mode

The PSU switches to turbining state at a certain period t, thus giving ξ^*=0, $\sum_{t=1}^{T} \alpha^*_t$ =1, so (13b) is satisfied.

For (13c), there are two possible cases: i) the PSU switches to the turbining state at period t for the first time. We have α^*_t=1, $\sum_{k=t+T^p-1}^{T} \beta^*_{tk}$ =1, and γ^*_{tk} =0. ii) Otherwise, we have α^*_t=0, $\sum_{k=t+T^p-1}^{T} \beta^*_{tk}$=1, and γ^*_{kt}=1. Thus, (13c) is satisfied.

For (13d), after switching to the pumping state at period t+1, there are two possible cases: i) the PSU keeps pumping from period t+1 to the end. We have $\sum_{k=1}^{T-T^q+1} \beta^*_{tk}$=1, θ^*_t =1, and $\sum_{k=t+T^q+1}^{T} \gamma^*_{tk}$=0. ii) the PSU switches to the turbining state at period k (t+T^{off}+1≤k≤T). We have $\sum_{k=1}^{T-T^q+1} \beta^*_{tk}$=1, θ^*_t =0, and $\sum_{k=t+T^q+1}^{T} \gamma^*_{tk}$=1. For both cases, (13d) is satisfied.

For (13e), if the PSU is turbining during the time interval (k,t), t∈[T-T^q, T], it will keep pumping during (t+1,T) due to the minimum-up constraints. Therefore, θ^*_t=1 and $\sum_{k=1}^{T-T^q+1} \beta^*_{tk}$=1.

(13e) is satisfied.

Constraints (13f)–(13z) and (1e)-(1m) both limit the continuous decision variables of PSU-1UC. Since P_t^*, Q_t^*, U_t^{u*}, U_t^{d*} meet (1e)-(1m), and $p_{tk,s}^*$, $q_{tk,s}^*$, $\vartheta_{tk,s}^{d*}$, $\vartheta_{tk,s}^{u*}$, $o_{tk,s}^{d*}$, $o_{tk,s}^{u*}$ are determined by P_t^*, Q_t^*, U_t^{u*}, U_t^{d*}, constraints (13f)–(13z) are satisfied with $p_{tk,s}^*$, $q_{tk,s}^*$, $\vartheta_{tk,s}^{d*}$, $\vartheta_{tk,s}^{u*}$, $o_{tk,s}^{d*}$, $o_{tk,s}^{u*}$.

To sum up, under any linear or piecewise-linear objective function, the optimal solution of the model (1) is a feasible solution of the model (13).

Optimality: The constructed feasible solution of the model (13) is also the following optimal solution

$$\sum_{t=1}^{T} C^{up}\alpha_t^* + \sum_{t=1}^{T}\sum_{k=t+T^p-1}^{T-1} C^{dn}\beta_{tk}^* + \sum_{t=T^p}^{t-T^q-1}\sum_{k=t+T^q+1}^{T} C^{up}\gamma_{tk}^* + \sum_{tk\in G}\sum_{s=t}^{k}\kappa_{tk,s}^{p*} + \sum_{tk\in H}\sum_{s=t}^{k}\kappa_{tk,s}^{q*} \tag{15}$$

Since $\kappa_{tk}^{qs} \ge \pi q_{tk}^{s}$, $\kappa_{tk}^{ps} \ge a^p p_{tk}^{s} + b^p \zeta_{tk}$, and the model (13) is a minimization problem, we have

$$\begin{cases} \sum_{tk\in G}\sum_{s=[t,k]} \kappa_{tk,s}^{p*} = \sum_{tk\in G}\sum_{s=[t,k]} a^p p_{tk,s}^* + b^p \zeta_{tk}^* = \sum_{tk\in G} P(t,k) \\ \sum_{tk\in G}\sum_{s=[t,k]} \kappa_{tk,s}^{q*} = \sum_{tk\in G}\sum_{s=[t,k]} \pi p_{tk,s}^* = \sum_{tk\in G} Q(t,k) \end{cases} \tag{16}$$

1) The first mode

If the optimal states are pumping for all the periods, we have

$$(15)=Q(1,T)=\Omega^-(0)=z \tag{17}$$

2) The second mode

If the optimal states are turbining for all the periods, we have

$$(15)=C^{up}+P(1,T)=C^{up}+\Omega^+(1)=\Omega^-(0)=z \tag{18}$$

3) The third mode

If the optimal states are to maintain the pumping state until period t_1-1, and then switch to the turbining state at period t_1, we have

$$\begin{aligned}(15) &= C^{up}\alpha_{t1} + \sum_{(t,k)\in\{(t,k)|\beta_{tk}^*=1\}} C^{dn} + \sum_{(t,k)\in\{(t,k)|\gamma_{tk}^*=1\}} C^{up} \\ &+ \sum_{(t,k)\in\{(t,k)|\beta_{tk}^*=1\}} P(t,k) + \sum_{(t,k)\in\{(t,k)|\psi_{tk}^*=1\}} Q(t,k) \\ &= Q(1,t_1-1)+C^{up}+\Omega^+(t_1)=\Omega^-(0)=z\end{aligned} \tag{19}$$

For both three operation modes, the optimal value of the LP model (13) and MIP model (1) is equal. As shown in Fig.3, the DP model (4) and the MIP model (1) both characterize the PSU-1UC problem, so they are two formulations of the PSU-1UC which are obviously equivalent. Moreover, the model (5) is the reformulation of the DP model (4). Meanwhile, the LP model (5) is equivalent to the model (13) based on the Strong Duality Theorem. Therefore, the LP model (13) is equivalent to the original MIP model (1), and the corresponding optimal value of the model (13) equals that of the model (1).

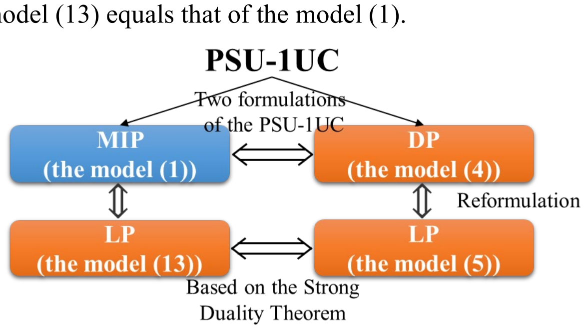

Fig.3 Relationship among the model (1), (4), (5), and (13)

From the above analysis, the optimal solutions of the model (1) and the model (13) are the same. Thus, the polyhedron provided by the model (13) is the convex hull of the model (1).

(Q.E.D)

Next, we construct the optimal solution for the decision variables (P_t^*, Q_t^*, x_t^*, u_t^*, U_t^{u*}, U_t^{d*}) of the model (1) according to the optimal solution (α_t^*, ξ^*, β_{tk}^*, γ_{tk}^*, θ_t^*, $p_{tk,s}^*$, $q_{tk,s}^*$, $\vartheta_{tk,s}^{d}$, $\vartheta_{tk,s}^{u}$, $o_{tk,s}^{d}$, $o_{tk,s}^{u}$) of the model (13).

Proposition 3: If (α_t^*, ξ^*, β_{tk}^*, γ_{tk}^*, θ_t^*, $p_{tk,s}^*$, $q_{tk,s}^*$, $\vartheta_{tk,s}^{d}$, $\vartheta_{tk,s}^{u}$, $o_{tk,s}^{d}$, $o_{tk,s}^{u}$) is the optimal solution of the model (13), we have

$$P_s^\dagger = \sum_{tk\in G, t\le s\le k} p_{tk,s}^*, \forall s\in[1,T] \tag{20a}$$

$$Q_s^\dagger = \sum_{tk\in H, t\le s\le k} q_{tk,s}^*, \forall s\in[1,T] \tag{20b}$$

$$x_s^\dagger = \sum_{tk\in G, t\le s\le k} \beta_{tk}^*, \forall s\in[1,T] \tag{20c}$$

$$u_s^\dagger = \alpha_s^* + \sum_{tk\in G, s=k} \gamma_{tk}^*, \forall s\in[1,T] \tag{20d}$$

$$U_s^{u\dagger} = \sum_{tk\in G, t\le s\le k} \vartheta_{tk,s}^{u*} + \sum_{tk\in H, t\le s\le k} o_{tk,s}^{u*}, \forall s\in[1,T] \tag{20e}$$

$$U_s^{d\dagger} = \sum_{tk\in G, t\le s\le k} \vartheta_{tk,s}^{d*} + \sum_{tk\in H, t\le s\le k} o_{tk,s}^{d*}, \forall s\in[1,T] \tag{20f}$$

where ($P_s^\dagger, Q_s^\dagger, x_s^\dagger$, $u_s^\dagger$, $U_s^{u\dagger}$, $U_s^{d\dagger}$) is the optimal solution of the MIP model (1).

Proof: We prove Proposition 3 from the two aspects: **feasibility** and **optimality**. Specifically, the variables $P_s^\dagger, Q_s^\dagger, x_s^\dagger, u_s^\dagger$, $U_s^{u\dagger}$, $U_s^{d\dagger}$ constructed by (20) are both the feasible and optimal solution of the model (1).

Feasibility:

4) For constraints (1b)-(1d)

Both $x_s^\dagger$ $u_s^\dagger$ are binaries and satisfy (1b) due to the definition of α_t^*, β_{tk}^*, γ_{tk}^*. Constraints (1c)-(1d) hold because the time pair (t,k) meet the minimum-up period limits.

5) For constraints (1e)-(1f)

Taking (20a)-(20c) into (1e), we have

$$\sum_{tk\in G, t\le s\le k} \beta_{tk}^* P^{\min} \le \sum_{tk\in G, t\le s\le k} p_{tk,s}^* \le \sum_{tk\in G, t\le s\le k} \beta_{tk}^* P^{\max}, \forall s\in[1,T] \tag{21}$$

Suppose that the PSU keeps turbining during the time interval (t', k'), (21) can be simplified to

$$\beta_{t'k'}^* P^{\min} \le p_{t'k',s}^* \le \beta_{t'k'}^* P^{\max}, \forall s\in[1,T] \tag{22}$$

Thus, (1e) is satisfied since (22) is equivalent to (13j). Similarly, (1f) is satisfied.

6) For constraints (1g)-(1h)

Taking (20a)-(20c) into (1g), we have

$$\begin{cases} \sum_{tk\in G, t=s} p_{tk,t}^* \le \overline{V^p} \sum_{tk\in G, s=t} \beta_{tk}^* \\ \left| \sum_{tk\in G, t+1\le s\le k} p_{tk,s}^* - \sum_{tk\in G, t+1\le s\le k} p_{tk,s-1}^* \right| \le V^p \sum_{tk\in G, t+1\le s\le k} \beta_{tk}^*, \forall s\in[1,T] \\ \sum_{tk\in G, t=k} p_{tk,k}^* \le \overline{V^p} \sum_{tk\in G, s=k} \beta_{tk}^* \end{cases} \tag{23}$$

Suppose that the PSU keeps turbining during the time interval (t',k'), (23) can be simplified to

$$\begin{cases} p^*_{t'k',t'} \le \overline{V^p} \\ \left|p^*_{t'k',s} - p^*_{t'k',s-1}\right| \le V^p \text{ ,} \forall s \in [1,T] \\ p^*_{t'k',k'} \le \overline{V^p} \end{cases} \quad (24)$$

Thus, (1g) is satisfied since (24) is equivalent to (13k) and (13l). Similarly, (1h) is satisfied.

7) For constraints (1i)-(1j)

Taking (20e)-(20f) into (1i), we have

$$\underline{U^u} \le \sum_{tk\in G, t\le s\le k} \vartheta^{u*}_{tk,s} + \sum_{tk\in H, t\le s\le k} o^{u*}_{tk,s} \le \overline{U^u}, s\in[1,T] \quad (25)$$

Suppose that the PSU keeps turbining or pumping during the time interval (t',k'), (25) can be simplified to

$$\begin{aligned} &\underline{U^u} \le \vartheta^{u*}_{t'k',s} \le \overline{U^u}, s\in[1,T] \\ &\underline{U^u} \le o^{u*}_{t'k',s} \le \overline{U^u}, s\in[1,T] \end{aligned} \quad (26)$$

Thus, (1i) is satisfied since (26) is equivalent to (13n). Similarly, (1j) is satisfied.

8) For constraints (1j)-(1k)

Taking (20a)-(20f) into (1k), we have

$$\begin{aligned} &\sum_{tk\in G, t\le s\le k} \vartheta^{u*}_{tk,s} + \sum_{tk\in H, t\le s\le k} o^{u*}_{tk,s} - \sum_{tk\in G, t\le s\le k} \vartheta^{u*}_{tk,s+1} - \sum_{tk\in H, t\le s\le k} o^{u*}_{tk,s+1} \\ &= \eta^p \sum_{tk\in G, t\le s\le k} p^*_{tk,s} + \eta^q \sum_{tk\in G, t\le s\le k} q^*_{tk,s}, \forall s\in[1,T-1] \end{aligned} \quad (27)$$

There are four possible cases of the PSU for (27):

i) pumping during [t', k'] and $s\in$ [t', k'-1], we have

$$\sum_{tk\in H, t\le s\le k} o^{u*}_{tk,s} - \sum_{tk\in H, t\le s\le k} o^{u*}_{tk,s+1} = \eta^q \sum_{tk\in G, t\le s\le k} q^*_{tk,s} \quad (28a)$$

ii) turbining during [t', k'] and $s\in$ [t', k'-1], we have

$$\sum_{tk\in G, t\le s\le k} \vartheta^{u*}_{tk,s} - \sum_{tk\in G, t\le s\le k} \vartheta^{u*}_{tk,s+1} = \eta^p \sum_{tk\in G, t\le s\le k} p^*_{tk,s} \quad (28b)$$

iii) pumping during [t', k'] and s=k', we have

$$\sum_{tk\in H} o^{u*}_{tk,k} - \sum_{(k+1,t)\in G} \vartheta^{u*}_{(k+1,t),k+1} = \eta^q \sum_{tk\in G} q^*_{tk,k} \quad (28c)$$

iv) turbining during [t', k'] and s=k', we have

$$\sum_{tk\in G} \vartheta^{u*}_{tk,k} - \sum_{tk\in H, t\le s\le k} o^{u*}_{(k+1,t),k+1} = \eta^p \sum_{tk\in G} p^*_{tk,k} \quad (28d)$$

where four constraints in (28) are equivalent to the constraints (13o), (13u), (13v), and (13w), respectively. Thus, (1j) is satisfied. Similarly, (1k) is satisfied.

To sum up, the solution (20) is a feasible solution of the original MIP model (1).

Optimality:

Taking (20) into (1a), we have

$$\begin{aligned} &\sum_{t=1}^{T} C^{up}\alpha^*_t + \sum_{t=1}^{T}\sum_{k=t+T^p-1}^{T-1} C^{dn}\beta^*_{tk} + \sum_{t=T^p}^{t-T^q-1}\sum_{k=t+T^q+1}^{T} C^{up}\gamma^*_{tk} \\ &+\sum_{tk\in G}\sum_{s=[t,k]} (a^p p^*_{tk,s} + b^p \zeta^*_{tk}) + \sum_{tk\in G}\sum_{s=[t,k]} \pi p^*_{tk,s} \end{aligned} \quad (28)$$

Formula (28) is the same as the optimal value of the model (13) (see formulas (15) and (16) in Proposition 2). Therefore, the solution (20) is an optimal solution of the MIP model (1).

(Q.E.D.)

Finally, the convex hull model of PSU-1UC can be precisely expressed as follows

$$\min \sum\nolimits_{t=1}^{T} (C^{up}u_t + C^{dn}(u_t + x_{t-1} - x_t) + f(P_t, Q_t, x_t)) \quad (29a)$$

s.t. (13b)-(13z), (20) (29b)

It is found that the convex hull model (28) is a simple single-level LP formulation, which can be easily solved by commercial solvers, such as CPLEX [24] and GUROBI [25]. Using the proposed convex hull model, the previous MIP model will be equivalent to an LP model without binary variables. This will significantly alleviate the computational burden and can be easily used to solve single-unit self-scheduling/ bidding problems or serve as a subproblem of the multi-unit commitment in decomposition algorithms.

Discussions: The proposed LP model provides the convex hull of the original MIP model for the PSU-1UC without any binary variables, which may have the following potential applications:

i) *PSU self-scheduling/bidding problems:* Comparing the original MIP model, the proposed LP model significantly reduces the time complexity from O($2^{2T}L$) to O(T^2L). Thus, it can be used to solve single-generator self-scheduling/bidding problems efficiently.

ii) *Decomposition algorithms for large-scale UC problems:* The decomposition algorithm for large-scale UC problems is a kind of iterative method. It requires solving the subproblem repeatedly until the optimal solution converges. Suppose that the reduced time of a single iteration is T^{single}, the total reduced time is $N\times T^{single}$, where N represents the iteration number. Taking the LR method as an example, N is usually more than 100, which is greater when the number of periods increases [26]. Therefore, formulating the subproblem as an LP instead of an MIP will significantly improve computational efficiency.

iii) *Nonconvex pricing in* the *electricity market:* Convex hull price (CHP) has attracted a lot of attention [17], [27]. Compared with the locational marginal price, CHP meets the incentive compatibility principle, which can effectively minimize the uplift payments. However, existing papers haven't reported the convex hull formulation for hydropower and energy storage units, while only studying the convex hull model for thermal power units. This paper first gives the convex hull formulation of PSUs in a single-unit UC, and the corresponding proof for the tightness. Thus, the CHP model can be easily extended to PSUs and other energy storage units.

IV. Case Study

In this section, we first analyze the compactness of the convex hull provided by the LP model (29). Then, the computational efficiency of both the original MIP model (1) and the LP model (29) is tested. Numerical results are conducted on a computer with 128 GB RAM and an Intel(R) Xeon(R) CPU E5-2650 processor, and all of the cases are solved by the commercial solver GUROBI 8.1.0.

A. Data description

The parameters are extracted from an actual PSU (i.e., the Siahbishe PSU in Iran) [28-29]. Specifically, the pumping power interval [Q^{min},Q^{max}] is [0,130]MW; the turbining power interval [P^{min},P^{max}] is [40,130]MW; the number of minimum-turbining/-pumping periods T^p/T^q is set to 6 hours (h); the ramp rate limits for the pump/turbine V^p/V^q are both set to 50MW/h; the conversion coefficient of water-to-electricity/electricity-to-water η^p/η^q is 0.75. In addition, a time series of electricity prices (T=24h) is shown in TABLE II.

TABLE II A Time Series of Electricity Prices (¥/MWh)

Period	1	2	3	4	5	6	7	8	9	10	11	12
Price	130	150	160	135	150	150	220	240	250	220	200	130

Period	13	14	15	16	17	18	19	20	21	22	23	24
price	120	125	130	160	260	280	250	220	200	160	130	130

B. Computational results of the day-ahead self-scheduling

Driven by the electricity prices in TABLE II, the optimal outputs and the corresponding reservoir volumes of the proposed LP model (29) are shown in Fig.4. It can be observed that the PSU is turbining during the time interval (6,10) and (16,20) under high electricity prices, and is pumping during the time interval (1,5), (11,15), and (21,24) when the electricity price is low. This verifies that the PSU can shift the net load by responding to the market price.

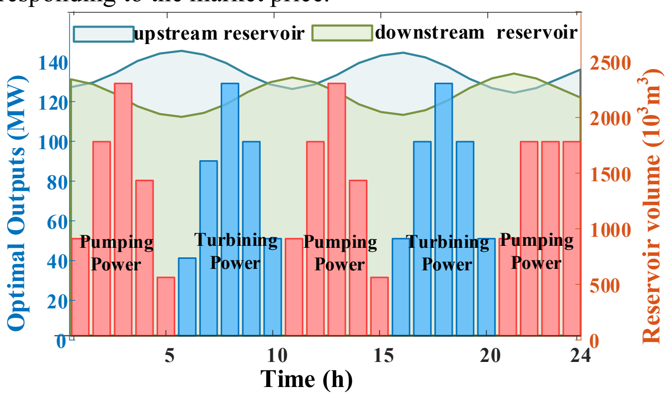

Fig.4 Optimal solution of the PSU-1UC

Then, we generate 100 groups of parameters (i.e., 100 samples) by adjusting the values of Q^{min}, Q^{max}, P^{min}, P^{max}, T^p, T^q within a certain range, and compare the relative errors of the LP model (29) and MIP model (1), where the relative error e is defined as

$$e = \frac{z^{\mathrm{LP}} - z^{\mathrm{MIP}}}{z^{\mathrm{MIP}}} \times 100\% \tag{30}$$

where z^{LP} denotes the optimal value of the LP model (29), and z^{MIP} represents the optimal value of the MIP model (1). The relative errors e of these 100 samples are shown in the frequency histogram (see Fig. 5). The maximum, minimum, and mean values of e are 1.49×10^{-4}%, 0.71×10^{-4}%, and 1.08×10^{-4}%, respectively. Each bar of the histogram represents the counts of the e within the corresponding interval. For example, there are 31 samples whose errors are within [0.85×10^{-4}%, 0.96×10^{-4}%]. According to the histogram, the normal distribution function of the relative error e is fitted as the red line in the figure. Its expectation μ and standard deviations σ are 1.077×10^{-4}% and 2.048×10^{-5}%, respectively. Based on the 3σ rule, 99.7% values of e are within [0.463×10^{-4}%, 1.691×10^{-4}%]. Therefore, the relative error e is small enough to be ignored, and the convex hull provided by the LP model (29) is compact.

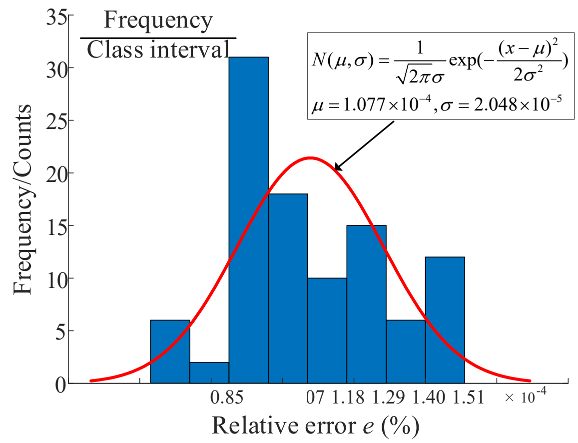

Fig.5 The frequency histogram of the relative error e

C. Computational efficiency of PSU-1UC

Next, the number of dispatching periods T is set to 48h, and the computational time of PSU-1UC with different T^p and T^q is tested. Denote the computational time of the MIP model and LP model by $\mathrm{T^{MIP}}$ and $\mathrm{T^{LP}}$, respectively. We analyzed the sensitivities of $\mathrm{T^{MIP}}$ and $\mathrm{T^{LP}}$ to T^p/T^q. For the LP model, Fig.6 depicts that, with T^p/T^q increasing from 5h to 45h, the number of constraints decreases from 21803 to 328, and $\mathrm{T^{LP}}$ decreases from 137ms to 2ms. This is because the scalability of the LP model depends on the cardinalities of the set G and H which are inversely proportional to T^p/T^q. While for the MIP model in TABLE III, $\mathrm{T^{MIP}}$ is about 200ms and is hardly affected by T^p and T^q. Therefore, the computational efficiency of the proposed LP model is higher than that of the MIP model, especially when T^p and T^q are large.

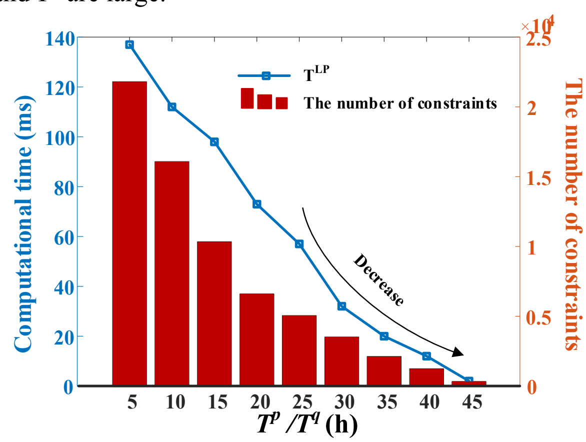

Fig.6 The number of constraints and $\mathrm{T^{LP}}$ of the LP model

TABLE III The number of constraints and $\mathrm{T^{LP}}$ of the MIP model

T^p/T^q(h)	5	10	15	20	25	30	35	40	45
Number of constraints	710	700	690	680	670	660	650	640	630
$\mathrm{T^{MIP}}$(ms)	220	208	217	198	206	217	200	186	224

Furthermore, the relationship among the model scales, computational time $\mathrm{T^{MIP}}/\mathrm{T^{LP}}$, and the number of periods T is analyzed. The model scales of the MIP model and the LP model are shown in TABLE IV, where NV and NC denote the numbers of variables and constraints, respectively; superscripts "MIP" and "LP" represent the MIP model and the LP model; subscripts "con" and "bin" denotes the number of continuous variables and binary variables, respectively. The results show that NV_{con}^{LP} is 2.1 to 9.4 times greater than NV_{con}^{MIP}. The number of constraints NC^{LP} is 4 to 18 times greater than NC^{MIP}. Thus, the scale of the LP model is larger than that of the MIP model.

TABLE IV Computational time of the convex hull model and MIP model under different system scales

T (h)	The LP model			The MIP model			
	NV_{con}^{LP}	NC^{LP}	T^{LP}(s)	NV_{bin}^{MIP}	NV_{con}^{MIP}	NC^{MIP}	T^{MIP}(s)
96	809	2301	0.01	288	384	576	0.015
168	1697	4834	0.03	504	672	1008	0.06
720	12088	4322	0.56	2160	2880	4320	1.52
2160	45367	129592	1.02	6480	8640	12960	2.89
4380	129135	368917	5.09	13140	17520	26280	18.11
8760	331141	946066	16.6	26280	35040	52560	62.26

Fig.7 shows the increase of T^{MIP} and T^{LP} with the increase of T. Specifically, when T increases from 96h to 8760h, T^{LP} increases from 0.01s to 16.63s, and T^{MIP} increases from 0.015s to 62.26s. The proportion of T^{MIP} to T^{LP} decreases from 67% to 27%. It is suggested that T^{MIP} grows faster than T^{LP}. This is because the LP model does not contain integer variables. While for the MIP model, the binary variables will make the feasible region discrete, resulting in a significant increase in computational time. Therefore, the computational efficiency of the LP model is much higher (33% - 73% in this case) than that of the MIP model, especially for the long-period UC problems.

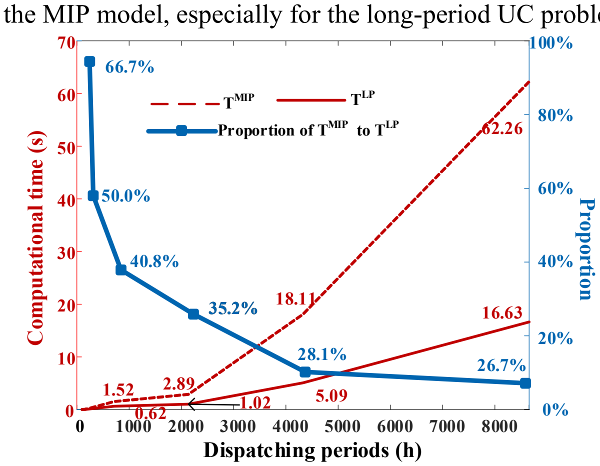

Fig. 7 Computational time of the convex hull model and MIP model

V. CONCLUSION

This paper proposes an efficient polynomial-time DP model for the PSU-1UC problem. Then, we construct an LP model of the PSU-1UC based on the proposed DP model, which provides the convex hull of the original MIP model. Simulation results show that the MIP model and LP model are equivalent. Moreover, the computational efficiency of the convex hull model is 33%-73% higher than that of the MIP model. In future work, the proposed convex hull model can be used to solve the PSU self-scheduling /bidding problems. Also, it helps to speed up the large-scale multi-UC problems solved by decomposed algorithms. In addition, the proposed convex hull model of PSU-1UC can be used to provide convex hull prices for hydropower and energy storage units.

REFERENCES

[1] Q. Zheng, J. Wang and A. L. Liu, "Stochastic Optimization for Unit Commitment—A Review," *IEEE Trans. Power Syst.*, vol. 30, no. 4, pp. 1913-1924, Jul. 2015.

[2] H. Abdi, "Profit-based unit commitment problem: A review of models, methods, challenges, and future directions," *Renew. Sust. Energ. Rev.*, vol. 138, p. 110504, Mar. 2021.

[3] S. Sen and D. P. Kothari, "Optimal thermal generating unit commitment: a review," *International Journal of Electrical Power & Energy Systems*, vol. 20, no. 7, pp. 443-451, Oct. 1998.

[4] Q. Gao, Z. Yang, W. Yin, W. Li and J. Yu, "Internally Induced Branch-and-Cut Acceleration for Unit Commitment Based on Improvement of Upper Bound," *IEEE Trans. Power Syst*, vol. 37, no. 3, pp. 2455-2458, May. 2022.

[5] Z. Guo, R. L. -Y. Chen, N. Fan and J. -P. Watson, "Contingency-Constrained Unit Commitment With Intervening Time for System Adjustments," *IEEE Trans. Power Syst.*, vol. 32, no. 4, pp. 3049-3059, Jul. 2017.

[6] J. M. Arroyo and A. J. Conejo, "Modeling of start-up and shut-down power trajectories of thermal units", *IEEE Trans. Power Syst.*, vol. 19, no. 3, pp. 1562-1568, Aug. 2004.

[7] M. Tahantn, W. van Ackooij, A. Frangioni, and F. Lacalandra, "Large-scale Unit Commitment under uncertainty," *4OR*, vol. 13, no. 2, pp. 115-171, Jun. 2015.

[8] Q. Zhai, X. Guan and J. Cui, "Unit commitment with identical units successive subproblem solving method based on Lagrangian relaxation," *IEEE Trans.Power Syst.*, vol. 17, no. 4, pp. 1250-1257, Nov. 2002.

[9] M. A. Bragin and P. B. Luh, "Distributed and asynchronous unit commitment and economic dispatch," *2017 IEEE Power & Energy Society General Meeting*, 2017, pp. 1-5.

[10] M. A. Bragin, P. B. Luh, J. H. Yan, N. Yu, and G. A. Stern, "Convergence of the Surrogate Lagrangian Relaxation Method," *J. Optimiz. Theory App.*, vol. 164, no. 1, pp. 173-201, Jan. 2015.

[11] P. Ramanan, M. Yildirim, E. Chow and N. Gebraeel, "An Asynchronous, Decentralized Solution Framework for the Large Scale Unit Commitment Problem", *IEEE Trans. Power Syst.*, vol. 34, no. 5, pp. 3677-3686, Sept. 2019.

[12] M. J. Feizollahi, M. Costley, S. Ahmed, and S. Grijalva, "Large-scale decentralized unit commitment," *Int. J. elec. power*, vol. 73, pp. 97-106, Dec. 2015.

[13] C. Wang and Y. Fu, "Fully Parallel Stochastic Security-Constrained Unit Commitment," *IEEE Trans. Power Syst.*, vol. 31, no. 5, pp. 3561-3571, Sept. 2016.

[14] R. H. Wuijts, M. van den Akker, and M. van den Broek, "An improved algorithm for single-unit commitment with ramping limits," *Electr. Pow. Syst. Res.*, vol. 190, p. 106720, Jan. 2021.

[15] F. Antonio and C. Gentile, "Solving non-linear single-unit commitment problems with ramping constraints," *Operations Research*, vol. 54, pp. 767-775, Jan. 2006.

[16] Y. Guan, K. Pan, and K. Zhou, "Polynomial-Time Algorithms and Extended Formulations for Unit Commitment Problems," *IISE Trans.*, vol.50, no.8, pp.735, 2018.

[17] Y. Yu, Y. Guan and Y. Chen, "An Extended Integral Unit Commitment Formulation and an Iterative Algorithm for Convex Hull Pricing," *IEEE Trans. Power Syst*., vol. 35, no. 6, pp. 4335-4346, Nov. 2020.

[18] B. Yan et al., "A Systematic Formulation Tightening Approach for Unit Commitment Problems," *IEEE Tran. Power Syst.*, vol. 35, no. 1, pp. 782-794, Jan. 2020.

[19] G. E. Alvarez, M. G. Marcovecchio, and P. A. Aguirre, "Security-Constrained Unit Commitment Problem including thermal and pumped storage units: An MILP formulation by the application of linear approximations techniques," *Electr. Pow. Syst. Res.*, vol. 154, pp. 67-74, Jan. 2018.

[20] Y. Zhou, Q. Zhai, W. Yuan, and J. Wu, "Capacity expansion planning for wind power and energy storage considering hourly robust transmission constrained unit commitment," *Appl. Energy*, vol. 302, p. 117570, Nov. 2021.

[21] K. Bruninx, Y. Dvorkin, E. Delarue, H. Pandžić, W. D'haeseleer and D. S. Kirschen, "Coupling Pumped Hydro Energy Storage With Unit Commitment," *IEEE Trans. Sustain. Energy*, vol. 7, no. 2, pp. 786-796, Apr. 2016.

[22] M. Reolon Scuzziato, E. Cristian Finardi, and A. Frangioni, “Solving stochastic hydrothermal unit commitment with a new primal recovery technique based on Lagrangian solutions,” *Int. J. elec. power*, vol. 127, p. 106661, May. 2021.
[23] N. Zhang et al., "Planning Pumped Storage Capacity for Wind Power Integration," *IEEE Trans. Sustain. Energy*, vol. 4, no. 2, pp. 393-401, Apr. 2013.
[24] https://www.ibm.com/analytics/cplex-optimizer
[25] .https://www.gurobi.com/
[26] Y. Fu, Z. Li and L. Wu, "Modeling and solution of the large-scale security-constrained unit commitment", *IEEE Trans. Power Syst.*, vol. 28, no. 4, pp. 3524-3533, Nov. 2013.
[27] D. A. Schiro, T. Zheng, F. Zhao and E. Litvinov, "Convex Hull Pricing in Electricity Markets: Formulation, Analysis, and Implementation Challenges," *IEEE Trans. Power Syst.*, vol. 31, no. 5, pp. 4068-4075, Sept. 2016.
[28] A. A. Salimi, A. Karimi, and Y. Noorizadeh, "Simultaneous operation of wind and pumped storage hydropower plants in a linearized security-constrained unit commitment model for high wind energy penetration," *J. Energy Storage*, vol. 22, pp. 318-330, Apr. 2019.
[29] Iran Water and Power Resources Development Company (IWPCo), http://en.iwpco.ir/Siahbishe/default.aspx